Exact Spin Liquid Ground States of the Quantum Dimer Model on the Square and Honeycomb Lattices

Hong Yao and Steven A. Kivelson

Phys. Rev. Lett. **108**, 247206 — Published 13 June 2012

DOI: 10.1103/PhysRevLett.108.247206

Exact Spin Liquid Ground States of the Quantum Dimer Model on the Square and Honeycomb Lattices

Hong Yao[1,2] and Steven A. Kivelson[1]

[1] *Department of Physics, Stanford University, Stanford, CA 94305, USA*
[2] *Institute for Advanced Study, Tsinghua University, Beijing, 100084, China*

(Dated: May 4, 2012)

We study a generalized quantum hard-core dimer model on the square and honeycomb lattices, allowing for first and second neighbor dimers. At generalized RK points, the exact ground states can be constructed, and ground-state correlation functions can be equated to those of *interacting* 1+1 dimensional Grassmann fields. When the concentration of second neighbor dimers is small, the ground state correlations are shown to be short-ranged corresponding to a (gaped) spin liquid phase. On a 2-torus, the ground states exhibit fourfold topological degeneracy. On a finite cylinder we have found a dramatic even-odd effect depending on the circumference, and propose that this can be used as a numerical diagnostic of gapped spin-liquid phases, more generally.

There has been a surge in numerical experiments [1–3] on simple models reporting evidence of the existence of fully gapped (short-ranged) spin-liquid states, including reports for the spin-1/2 Heisenberg model with first and second neighbor anti-ferromagnetic couplings (J_1 and J_2) on the square [3] and honeycomb [4] lattice as well as the Hubbard model on the honeycomb lattice[2]. For the square lattice model, an early numerical study[5] on a relatively small system was interpreted as evidence for a spin-liquid, but this result was seriously questioned on the basis of the results of series expansion[6], large-N[7], and large-S[8] studies of the same model. In the case of the honeycomb lattice, recent studies reported[2] evidence of such a state for an intermediate range of U/t in the Hubbard model. For both the square and honeycomb lattice, there is no solvable model with the same symmetries as the Heisenberg model for which a gaped spin-liquid state has been found. Having a caricature of the putative state is useful in thinking about the phase, and possibly also in designing numerical experiments to confirm or falsify its existence.

Here, we report a generalization of the quantum hard-core dimer model[9, 10] on the square and honeycomb lattices, for which the exact spin-liquid groundstates can be obtained for certain values of coupling constants dubbed as "generalized Rokhsar-Kivelson (RK) points". In the limit in which all dimers occupy nearest-neighbor links, this spin-liquid has critical ground-state correlations, and correspondingly gapless collective excitations[9, 11, 12]. However, when the dynamics are generalized to generate even a small concentration of second neighbor dimers, the ground-state correlations become short-ranged and a gap opens in the spectrum. Indeed, although the ground-state correlations in this limit can no longer be computed directly using Pfaffian methods[13], close to the critical point, where the concentration of second neighbor dimers is small, the correlations are asymptotically equivalent to those of a 1+1 dimensional massive Thirring model, and so are still exactly known[14].

In the course of this study, we have also recognized a new, possibly useful diagnostic tool for numerical searches for spin-liquids: We find the exact spin-liquid ground state on a torus with a finite circumference, L_y, spontaneously breaks translational symmetry (forms a "columnar" density wave state) for odd L_y, but is translationally invariant for even L_y. (A similar phenomenon occurs when a fractional quantum Hall fluid is considered in the narrow torus limit[15, 16].) For odd L_y, the amplitude of the columnar order parameter decays exponentially in proportion to $\frac{1}{L_y^{1/2}}\exp[-L_y/2\xi]$, where ξ is the dimer-dimer correlation length[17]. We note that a similar even-odd effect with exponential decrease in the amplitude of the columnar order parameter for odd L_y have been observed[3] in DMRG studies of the square-lattice spin-1/2 J_1-J_2 model on cylinders with $L_y = 3 - 10$.

Model: The quantum dimer model is defined on a Hilbert space with distinct, orthonormal states corresponding to each allowed hard-core dimer covering of the lattice. The Hamiltonian is defined by matrix elements between dimer states, with "potential" terms, V, V', $\lambda V''$, and V''/λ, which are diagonal in the dimer basis and associate an interaction energy with various local arrangements of dimers, and "kinetic" terms, t, t', and t'', which involve a local rearrangement of a small number of dimers. On the square lattice, we represent the Hamiltonian graphically as:

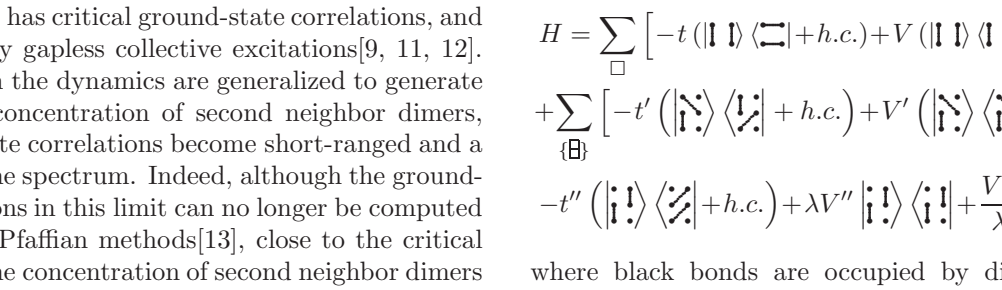

(1)

where black bonds are occupied by dimers, the first sum runs over all plaquettes, and the second and third over all pairs of adjacent plaquettes (with both orientations). The first line is Eq. (1) is the original quantum

dimer model on the square lattice with only first neighbor dimers[9]. The added terms are the shortest-range terms involving second-neighbor dimers. The parameter λ determines the relative preference for first and second-neighbor dimers.

A similar construction can be used to define the model on the honeycomb lattice:

$$H = \sum_{\hexagon} \Big[-t \left(|\rangle\langle| + h.c. \right) + V \left(|\rangle\langle| + |\rangle\langle| \right) - t' \left(|\rangle\langle| + h.c. \right) + V' \left(|\rangle\langle| + |\rangle\langle| \right) - t'' \left(|\rangle\langle| + h.c. \right) + \lambda V'' |\rangle\langle| + \frac{V''}{\lambda} |\rangle\langle| \Big] \quad (2)$$

where various parameters have similar meaning as in the case of square lattice, and it is implicit that all terms are to be summed over symmetry related orientations.

In defining these models, we have restricted the Hilbert space by excluding configurations with crossed dimers. We do this for two reasons: Firstly, more microscopically, the dimers are thought to be representations of spin singlets (or valence bonds) which are assumed to be the building blocks of the low energy subspace of an underlying quantum spin 1/2 problem with strong frustration. However, there are only two linearly independent singlet states corresponding to four spin 1/2's on a plaquette, or in other words, if we identify dimer configurations with orthogonalized versions of valence bond states, then $|\rangle \propto -(|\rangle + |\rangle)$. (It is an open question whether the remaining states with first and non-crossing second neighbor valence bonds are linearly independent[18].) Secondly, for the model as defined, crossed dimers would be non-dynamical unless we were to include additional terms in the Hamiltonian.

For the system with a torus or cylinder geometry, it is known that dimer configurations can be classified according to topological labels or winding numbers; dimer configurations with different winding numbers cannot be connected by local moves of dimers. On the square and honeycomb lattices, configurations with only first neighbor dimers are characterized by integer winding numbers[9] due to the bipartiteness of the model. However, for the dimer configurations allowing both first and second neighbor dimers, the bipartiteness is lost and on a 2-torus there are only four topological sectors labeled by $W = (W_x, W_y)$, where W_i is odd or even. A simple way to determine W_x is to draw a vertical line across the whole system and see how many dimers it cuts whose parity is then W_x, and W_y is defined similarly in terms of the even or oddness of the number of dimers crossing a horizontal line. More generally, the number and character of the topological sectors depends on the boundary conditions in ways that are straightforward to determine.

The RK point: For generic parameters the exact ground state is not known. However, at the so-called Rohksar-Kivelson (RK) points, exact ground states of both the models can be determined explicitly. For both Hamiltonians [Eq. (1) and Eq. (2)], the generalized RK points are given by

$$t = V,\ t' = V',\ \text{and}\ t'' = V'', \quad (3)$$

and any finite λ. At these RK points, both Eq. (1) and Eq. (2) can be expressed as a sum of projection operators and can thus be shown to be positive semi-definite[9], with groundstates:

$$|\Psi_0\rangle = \sum_c \lambda^{n_s(c)/2} |c\rangle\,, \quad (4)$$

where the summation is over all dimer configurations, c, in a given topological sector and $n_s(c)$ is the number of second-neighbor dimers in c. That this is an exact ground-state can be seen by explicitly checking that it is anihilated by the Hamiltonian [Eq. (1) or Eq. (2)]. On the torus, there are four sectors so the ground states have fourfold topological degeneracy[19, 20].

It remains to characterize the phases described by these exact ground-states in terms of the behavior of the dimer-dimer correlation functions. For the RK wave function with only first neighbor dimers, the ground state is known to correspond to a quantum multi-crtical point with power-law decay of correlation functions. However, as we shall show, the wave function described by Eq. (4) is more akin to that of the dimer model on the triangular lattice in the sense that all groundstate correlation functions fall exponentially with distance[21].

Path integral representation: The dimer-dimer correlation function in a ground state RK wave function $|\Psi_0\rangle$ is defined as

$$\langle D_{ij} D_{i'j'} \rangle \equiv \frac{\langle \Psi_0 | D_{ij} D_{i'j'} |\Psi_0\rangle}{\langle \Psi_0 | \Psi_0 \rangle}, \quad (5)$$

where D_{ij} denote dimer operators on the link (ij) which is 1 when the link is occupied by a dimer and 0 otherwise. This is equivalent to the correlations of a classical dimer model in which the wave function normalization, $Z = \langle \Psi_0 | \Psi_0 \rangle$, plays the role of the partition

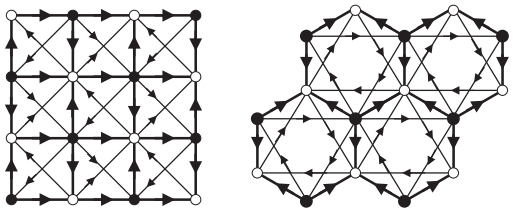

(a) (b)

FIG. 1. The arrow pattern on on the square and honeycomb lattices used in defining the Grassmann path integral representation of the classical dimer model. The black and white sites are the two sublattices.

function. For wave functions involving only first neighbor dimers, it is known that dimer densities and dimer-dimer correlation functions can be computed in terms of a path integral representation of non-interacting Grassmann fields, since a consistent arrow pattern determining the action of Grassmann fields is always possible for a planar graph[13]. Due to the appearance of second neighbor dimers, the graph is no longer planar and the Pfaffian method does not work directly. Nonetheless, the partition function can still be *exactly* expressed by the following path integral representation of *interacting* Grassmann fields (see the proof in Appendix):

$$Z = \int [da] e^{-S}, \tag{6}$$

$$S = \sum_{ij} i t_{ij} a_i a_j + \sum_{\langle ijkl \rangle} (i t_{ij} a_i a_j)(i t_{kl} a_k a_l), \tag{7}$$

where a_i are Grassmann numbers and $[da] = \prod_{i=1}^{N} da_i$ (N is the number of sites), $t_{ij} = \pm 1$ on the first neighbor links, $t_{ij} = \pm\lambda$ on second neighbor links, and $\langle ijkl \rangle$ denotes a pair of crossing second neighbor links ij and kl. Here, the sign of t_{ij} is determined from the pattern of arrows shown in Fig. 1, such that t_{ij} is positive if the arrow on the link (ij) points from i to j, and negative if it points from j to i. (The choice of a particular pattern of arrows amounts to a choice of gauge.)

Since the new thing here is the four-field "interaction" term, it worth discussing its origin heuristically. In the absence of the interaction term, the path integral has a contribution from dimer configurations with crossed dimers with an associated amplitude factor, $[-t_{ij}t_{kl}]$, which can be negative. The interaction term likewise generates crossed dimers with an amplitude $t_{ij}t_{kl}$, which is just what is needed to cancel the spurious term in the absence of interactions. The proof is in Appendix.

Massive Thirring model: The path integral in Eq. (6) describes the classical dynamics of fermionic fields in 2 spatial dimensions which can be mapped to a 1+1 dimensional quantum theory by treating one spatial dimension, say y, as time t.

For the square lattice, the arrow pattern we have chosen doubles the unit cell; for the honeycomb lattice, the unit cell already contains two sites, and no further increase is necessary in order to define a consistent pattern of arrows; we will thus define a new two-component field with a pseudo-spin index, α, which labels the sublattice. Translation symmetry allows us to block diagonalize the non-interacting part of the Hamiltonian by Fourier transform in terms of a new set of *complex* Grassmann fields

$$b_{\vec{k},\alpha} = \sqrt{\frac{1}{N}} \sum_{j \in \alpha} e^{i\vec{k}\cdot\vec{r}_j} a_j, \tag{8}$$

where $b^\dagger_{\vec{k},\alpha} = b_{-\vec{k},\alpha}$, since a_j are real Grassmann fields. The non-interacting part of the action is then

$$S_0 = \sum_{\vec{k} \in \frac{1}{2}\mathrm{BZ}} b^\dagger_{\vec{k}} h_{\vec{k}} b_{\vec{k}}, \tag{9}$$

where the sum runs over only half the Brillouin zone (See Fig. 2.) (since we have combined real fields with $\vec{k}$ and $-\vec{k}$ into a single complex field), and

$$h_{\vec{k}} = 2 \begin{bmatrix} 2\lambda \cos k_x \sin k_y & -\sin k_x + i \cos k_y \\ -\sin k_x - i \cos k_y & -2\lambda \cos k_x \sin k_y \end{bmatrix} \tag{10}$$

and

$$h_{\vec{k}} = \sum_{j=1}^{3} \begin{bmatrix} 2\lambda \sin[\vec{k}\cdot(\hat{e}_{j+1} - \hat{e}_j)] & i e^{i\vec{k}\cdot\hat{e}_j} \\ -i e^{-i\vec{k}\cdot\hat{e}_j} & -2\lambda \sin[\vec{k}\cdot(\hat{e}_{j+1} - \hat{e}_j)] \end{bmatrix},$$

for the square and honeycomb lattice, respectively. Here $\hat{e}_j$ are the vectors connecting first neighbors of the honeycomb lattice: $\hat{e}_1 = (0, -1)$, $\hat{e}_2 = (\sqrt{3}/2, 1/2)$, $\hat{e}_3 = (-\sqrt{3}/2, 1/2)$, and $\hat{e}_{j+3} \equiv \hat{e}_j$.

When $\lambda = 0$, the spectrum of $h_{\vec{k}}$ is gapless and has a single Dirac point at a momentum labeled $\vec{K}$ (the dot points in Fig. 2) within the half Brillouin zone: $\vec{K} = (0, \pi/2)$ for the square and $\vec{K} = (4\pi/3\sqrt{3}, 0)$ for the honeycomb lattice. A finite λ opens up a gap in the spectrum and is the mass term of the Dirac fermions. Indeed, taking the continuum limit of Eq. 9 for small λ produces a formal equivalence to the 1+1 D Dirac action:

$$S_0 = v_F \int dx dy \psi^\dagger [i\partial_y \sigma^x - i\partial_x \sigma^y + m_0 \sigma^z] \psi, \tag{11}$$

where for the square lattice, $v_F = 2$ and $m_0 = 2\lambda$ while for the honeycomb lattice, $v_F = \frac{3}{2}$ and $m_0 = 2\sqrt{3}\lambda$. Here $\psi_\alpha(\vec{r})$ is the slowly varying piece of the inverse Fourier transform of $b_{\vec{k},\alpha}$, with the rapidly oscillating factor, $\exp[i\vec{K}\cdot\vec{r}]$, removed. For small λ, the interaction term can also be treated in the naive continuum limit, so

$$S \to S_0 - g \int dx dy \psi^\dagger_1 \psi_1 \psi^\dagger_2 \psi_2. \tag{12}$$

where $g = 8\lambda^2$ for the square lattice and $g = 24\lambda^2$ for the honeycomb is the strength of attractive interaction. The effective interaction is attractive as it serves to cancel the (negative) weight for crossed dimers generated by S_0.

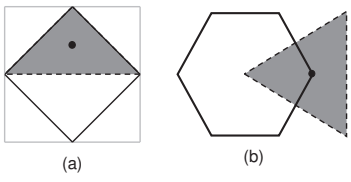

FIG. 2. The Brillouin zone (BZ) for the square and honeycomb lattices: The solid lines mark the boundaries of the full BZ corresponding to the arrow patterns in Fig. 1, with two sites per unit cell. The shaded area is the "half BZ" over which the $\vec{k}$-sum in Eq. 9 is carried out. The dot indicates the location of the Dirac node, $\vec{K}$, in the limit $\lambda \to 0$.

Rescaling the spatial coordinates so that $v_F = 1$, identifying y with the imaginary time, t, and introducing the notation $\bar{\psi} = \psi^\dagger \sigma^z$, we see that Eq. (12) is precisely the Euclidean action of the massive Thirring model. The massive Thirring model is, in turn, exactly solvable by Bethe ansatz[14]. The mass is renormalized as:

$$m \approx m_0 e^{-g/v_F \pi}. \tag{13}$$

In other words, the mass gap gets renormalized down but survives under weak attractive interactions. Indeed, the effect of interactions is only perturbative and does not qualitatively change the feature of the non-interacting model, as long as λ is small, *i.e.*, $\lambda^2 \log(\frac{1}{\lambda}) \ll 1$.

The finite gap in the spectrum at small but finite λ implies that the ground state dimer correlations are short-ranged[22]. Consequently, the ground states are gapped Z_2 quantum spin liquids with a fourfold topological degeneracy on a torus [23]. This is our central result.

Even-odd effect: Unambiguously identifying gapped spin-liquid phases is notoriously difficult experimentally since spin-liquid ground states exhibit no conventional broken symmetries. In this context, we note that when a system with a gapped spin-liquid groundstate is placed on a torus with a finite odd-length circumference L_y in one direction, a two-fold degenerate density-wave state (*i.e.* which spontaneously breaks translational symmetry) necessarily arises. However, the density wave order vanishes when L_y is even. This even-odd effect is rooted in the seminal theorem of Lieb, Schultz and Mattis[24, 25]: For a 1D system with an odd number of electrons per unit cell, there must always exist a distinct state with momentum π relative to the ground-state whose energy approaches arbitrarily close the ground state energy in the thermodynamic limit. (This theorem can be applied to the quantum dimer model by associating each dimer with a singlet pair of electrons [9].) Applying the Lieb-Schultz-Mattis theorem to gapped spin-liquids, one concludes that this ground-state degeneracy must correspond to translational symmetry breaking for L_y odd.

We have calculated the density-wave order parameters for various quantum dimer models on a torus of finite circumference L_y. In all cases, the density-wave order vanishes for even L_y. However, for odd and large L_y, we find columnar order which decays as $L_y^{-1/2} \exp[-L_y/2\xi]$, where ξ is the dimer-dimer correlation length in 2D. For the square lattice with small λ, the columnar density-wave order parameter $C(L_y)$ (defined as the difference between strong and weak bonds) is

$$C(L_y) \approx 2\sqrt{\frac{4\lambda(1-4\lambda^2)}{\pi(1-8\lambda^2)}} \left[\frac{e^{-(L_y+1)/2\xi}}{\sqrt{L_y+1}} + \frac{e^{-(L_y-1)/2\xi}}{\sqrt{L_y-1}} \right],$$

for $L_y \gg \xi$, where $\xi \approx 1/(4\lambda)$. Both the even-odd effect and exponential decay of the columnar order with increasing L_y have been observed in DMRG studies of the spin-1/2 J_1-J_2 Heisenberg model on a square lattice[3].

We have obtained similar even-odd results for the models on the triangular and Kagome lattices. Because the honeycomb lattice has two sites per unit cell, it is necessary to introduce twisted boundary conditions in order to have a torus with odd L_y. This twist globally lifts the degeneracy between the two, distinct columnar states. None-the-less, the magnitude of the bond alternation decays exponentially with increasing L_y in this case, as well.

Remark: The present results hold only for small λ. In the limit that $\lambda \to \infty$, the ground state has only second neighbor dimers and the system prefers to order by spontaneously breaking lattice symmetries.

Acknowledgement: We would like to thank Paul Fendley, Eduardo Fradkin, Hongchen Jiang, Dunghai Lee, Roderich Moessner, Shivaji Sondhi, and Weifeng Tsai for inspiring discussions. This work is partly supported by NSF Grants DMR-0904264 (H.Y.) and DMR-0758356 (S.A.K.).

[1] S. Yan, D. A. Huse, and S. R. White, Science **332**, 1173 (2011).

[2] Z. Y. Meng, T. C. Lang, S. Wessel, F. F. Assaad, and A. Muramatsu, Nature **464**, 847 (2010); D. Zheng, G.-M. Zhang, and C. Wu, Phys. Rev. B 84, 205121 (2011).

[3] H.-C. Jiang, H. Yao, and L. Balents, arXiv:1112.2241.

[4] B. K. Clark, D. A. Abanin, and S. L. Sondhi, Phys. Rev. Lett. **107**, 087204 (2011).

[5] F. Figueirido, A. Karlhede, S. Kivelson, S. Sondhi, M. Rocek, and D. S. Rokhsar, Phys. Rev. B **41**, 4619 (1990).

[6] M. P. Gelfand, R. R. P. Singh, and D. A. Huse, Phys. Rev. B **40**, 10801 (1989).

[7] N.Read and S.Sachdev, Phys. Rev. Lett. **62**, 1694 (1989).

[8] P. Chandra, P. Coleman, and A. I. Larkin, J. Phys. Condens. Matter **2**, 7933 (1990).

[9] D. S. Rokhsar and S. A. Kivelson, Phys. Rev. Lett. **61**, 2376 (1988).

[10] R. Moessner and S. L. Sondhi, Phys. Rev. Lett. **86**, 1881 (2001).

[11] E. Ardonne, P. Fendley, and E. Fradkin, Ann. Phys. **310**, 493 (2004).

[12] E. Fradkin, D. A. Huse, R. Moessner, V. Oganesyan, and S. L. Sondhi, Phys. Rev. B **69**, 224415 (2004).

[13] P. W. Kasteleyn, Physica **27**, 1209 (1961); H. N. V. Temperley and M. E. Fisher, Philos. Mag. **6**, 1061 (1961).

[14] H. Bergknoff and H. B. Thacker, Phys. Rev. Lett. **42**, 135 (1979).

[15] E. J. Bergholtz and A. Karlhede, J. Stat. Mech. (2006) L04001.

[16] A. Seidel and D.-H. Lee, Phys. Rev. Lett. **97**, 056804 (2006).

[17] Away from solvable points, the power-law prefactor may change to a $(2+z)$-dimensional Ornstein-Zernicke form.

[18] J. Wildeboer and A. Seidel, Phys. Rev. B **83**, 184430 (2011).

[19] S. A. Kivelson, D. S. Rokhsar, and J. Sethna, Phys. Rev. B **35**, 8865 (1987).

[20] X.-G. Wen, Phys. Rev. B **40**, 7387 (1989).

[21] A. W. Sandvik and R. Moessner, Phys. Rev. B **73**, 144504 (2006).

[22] P. Fendley, R. Moessner, and S. L. Sondhi, Phys. Rev. B **66**, 214513 (2002).

[23] R. Moessner, S. L. Sondhi, and E. Fradkin, Phys. Rev. B **65**, 024504 (2001).

[24] E. Lieb, T. Schultz and D. Mattis, Ann. Phys. **16**, 407 (1961).

[25] G. Misguich, C. Lhuillier, M. Mambrini, and P. Sindzingre, Eur. Phys. J. B **26**, 167 (2002).